AIAA JOURNAL
Vol. 34, No. 1, January 1996

Integrated Optimum Design of Structure and H^∞ Control System

K. Tsujioka,* I. Kajiwara,† and A. Nagamatsu‡
Tokyo Institute of Technology, Tokyo 152, Japan

An approach for an integrated optimum design of a structure and an H^∞ control system is presented. The complex method and the genetic algorithm are adopted in the optimization process in the integrated design. The structural shape and the control system, including the locations of both sensors and actuators, are optimized simultaneously by the proposed approach. The improvement of frequency response shaping under the constraint of the structural mass can be realized by the integrated optimum design presented in this paper. The desired properties with respect to the control performance and the robustness are realized by the frequency shaping ability of H^∞ control. Effectiveness of the presented approach is verified by both simulation and experiment by the integrated design of a panel structure and H^∞ control system.

Nomenclature

C = damping matrix of the original model $\in \boldsymbol{R}^{n\times n}$
d = number of disturbances
e = number of controlled variables
f = fitness function in genetic algorithm
$G(s)$ = transfer function matrix
g = DOF of the reduced modal model
J = objective function
K = stiffness matrix of the original FEM model $\in \boldsymbol{R}^{n\times n}$
$K(s)$ = H^∞ controller
M = mass matrix of the original FEM model $\in \boldsymbol{R}^{n\times n}$
n = DOF of the original FEM model
p = number of control inputs
$\boldsymbol{q}_s$ = state variable vector of the reduced modal model $\in \boldsymbol{R}^{2g}$
t = number of outputs
t_i = gene in GA
$\boldsymbol{u}$ = control force vector $\in \boldsymbol{R}^p$
$W(s)$ = frequency weighting function matrix
$\boldsymbol{w}$ = disturbance vector $\in \boldsymbol{R}^d$
w_i = modal weighting coefficient, $i = 1 \sim g$
$\boldsymbol{x}$ = displacement vector $\in \boldsymbol{R}^n$
$\boldsymbol{y}$ = output vector $\in \boldsymbol{R}^t$
$\boldsymbol{z}$ = controlled variable vector
Γ = reduced eigenvalue matrix $\in \boldsymbol{R}^{g\times g}$
γ = H^∞ norm of the transfer function matrix
$\boldsymbol{\xi}$ = reduced modal displacement vector $\in R^g$
τ = design variable vector of structure
Φ = reduced modal matrix $\in \boldsymbol{R}^{n\times g}$
Ω_i = ith-order natural frequency of structure, $i = 1 \sim g$

Introduction

In machines, such as optical disk devices and large flexible space structures, the characteristics of both the structure and the control system extensively influence each other. The optimum design of both the structure and the control system is required to realize improved performance in such kinds of machines. Results have been reported with respect to simultaneous optimization of the structure and the control system. The objective function has been defined as the combination of the structural and the control characteristics.[1] Computational aspects of the simultaneous optimization using a simple beam model have been shown as an example.[2] A method of vibration control of flexible space structures by simultaneously integrating structural design and control design has been provided, in which structural modification of a simple truss was performed using a finite element model (FEM) for optimal control by a linear regulator.[3] Structural modeling and optimum control of space structures have been studied,[4] and the structural and control design process of large-scale structures by linear regulator theory has been examined.[5] Iteration methods on optimum structure/control design for preventing vibrations of flexible structures have been proposed.[6,7] The sensitivity of a control system with respect to minor structural modifications has been discussed for combined control/structural design.[8] An approach to simultaneous optimum design of a structure and a control system for a large flexible spacecraft has been proposed.[9] A method for simultaneous optimization that assures the stability of the system corresponding to high-order natural modes that have been ignored in designing the control system has been given by the present authors.[10]

In the simultaneous optimization of actual complex structures, the stability robustness with respect to structural uncertainty is required in the design of the machines. An approach for the minimum weight design using H^∞ control theory has been presented.[11] The integrated optimum design of the structure and H^∞ control system to improve the frequency response shaping, however, has not been discussed enough.

In the present study, an approach for integrated optimum design of a structure and H^∞ control system is proposed. H^∞ control theory enables us to design a robust control system for a structure with parameter uncertainties. The desired properties of both the control performance and the robustness are realized by the frequency shaping ability of H^∞ control. Higher performance of frequency response shaping is achieved by integrated optimum design of the structure and H^∞ control system. Two optimization methods are adopted in this paper, namely, the complex method and the genetic algorithm (GA).

In the approach based on the complex method, a nonlinear optimization method, the objective function is the H^∞ norm of the closed-loop system that is the performance index of control. The structure is modeled by the finite element method and the model reduction is achieved through the use of modal coordinates. The shape of the FEM and a control parameter with respect to the H^∞ norm are adopted as design variables. As the existence of the solution of the H^∞ controller depends on the given H^∞ norm, this existence condition cannot be described as continuous function with respect to design variables. Thus, the complex method with which

Received Feb. 7, 1995; presented as Paper 95-1483 at the AIAA/ASME/ASCE/AHS/ASC 36th Structures, Structural Dynamics, and Materials Conference, New Orleans, LA, April 10–12, 1995; revision received July 19, 1995; accepted for publication July 19, 1995.

*Research Associate, Department of Mechanical Engineering and Science.
†Research Associate, Department of Mechanical Engineering and Science. Member AIAA.
‡Professor, Department of Mechanical Engineering and Science. Member AIAA.

the discontinuous objective function can be optimized is adopted in this approach.

In the approach based on GA, the size and the shape are adopted as the structural design variables, and the locations of the sensors and the actuators are adopted as the control design variables. As the sensors and the actuators are placed only at the nodal points of the FEM, the control design variables take the discrete values. GA is useful to search the optimum design variables in such a discontinuous problem. The frequency responses are shaped by the frequency weighting functions included in the H^∞ control system, and the modal weighting coefficients proposed in this paper. Adopting the modal weighting coefficient, the dynamic response of all natural modes can be controlled without increasing the order of the controller. The effectiveness and practicability of the proposed approach are verified by both simulation and experiment for controlling the vibration of a panel structure.

Modeling of System

Modeling of Structure

The original FEM spatial model of an n-degree-of-freedom (DOF) structure has the following equation of motion:

$$M\ddot{x} + C\dot{x} + Kx = B_{s1}w + B_{s2}u \tag{1}$$

The spatial matrices M and K are composed by FEM. As n is large in usual FEM structural models, Eq. (1) cannot be used directly for designing the control system. The equation of motion of this physical model is transformed from the spatial coordinate to the modal coordinate with $g(\ll n)$ natural modes in order to reduce the order of the model. Adopting the lower g normalized natural modes $\Phi \in \boldsymbol{R}^{n\times g}$, Eq. (1) is transformed to the reduced modal model with the following equation:

$$x = \Phi\xi \tag{2}$$

where $\Phi^T M\Phi = I_g$.

The state equation of the reduced modal model becomes

$$\dot{q}_s = A_s q_s + B_{1s}w + B_{2s}u \tag{3}$$

where

$$q_s = \begin{Bmatrix}\xi\\ \dot{\xi}\end{Bmatrix}, \quad A_s = \begin{bmatrix}0 & I_g\\ -\Gamma & -L\end{bmatrix}, \quad B_{1s} = \begin{bmatrix}0\\ \Phi^T B_{s1}\end{bmatrix}$$

$$B_{2s} = \begin{bmatrix}0\\ \Phi^T B_{s2}\end{bmatrix}, \quad L = \Phi^T C\Phi$$

The diagonal eigenvalue matrix Γ of this reduced modal model is defined as $\mathrm{diag}(\Omega_1^2, \Omega_2^2, \ldots, \Omega_g^2) \in \boldsymbol{R}^{g\times g}$.

The controlled variable $z_s \in \boldsymbol{R}^e$ is given by

$$z_s = C_{1s}q_s + D_{11s}w + D_{12s}u \tag{4}$$

where $C_{1s} \in \boldsymbol{R}^{e\times 2g}$, $D_{11s} \in \boldsymbol{R}^{e\times d}$, and $D_{12s} \in \boldsymbol{R}^{e\times p}$. The spatial output $y \in \boldsymbol{R}^t$ is given by

$$y = C_{2s}q_s + D_{21s}w + D_{22s}u \tag{5}$$

where $C_{2s} \in \boldsymbol{R}^{t\times 2g}$, $D_{21s} \in \boldsymbol{R}^{t\times d}$, and $D_{22s} \in \boldsymbol{R}^{t\times p}$. Equations (3–5) are synthetically formulated as

$$G_s(s) \triangleq \left[\begin{array}{c|cc} A_s & B_{1s} & B_{2s}\\ \hline C_{1s} & D_{11s} & D_{12s}\\ C_{2s} & D_{21s} & D_{22s}\end{array}\right] \tag{6}$$

where the notation

$$\left[\begin{array}{c|c} A & B\\ \hline C & D\end{array}\right] \triangleq C(sI - A)^{-1}B + D$$

is used in Eq. (6).

Frequency Shaping by Frequency Weighting Function

The frequency weighting functions with respect to the controlled variables are defined to shape the frequency responses:

$$z = W(s)z_s, \qquad W(s) \triangleq \left[\begin{array}{c|c} A_w & B_w\\ \hline C_w & D_w\end{array}\right] \tag{7}$$

The augmented state equation is obtained by synthesizing Eqs. (6) and (7),

$$G(s) \triangleq \left[\begin{array}{cc|cc} A_s & 0 & B_{1s} & B_{2s}\\ B_wC_{1s} & A_w & B_wD_{11s} & B_wD_{12s}\\ \hline D_wC_{1s} & C_w & D_wD_{11s} & D_wD_{12s}\\ C_{2s} & 0 & D_{21s} & D_{22s}\end{array}\right] = \left[\begin{array}{c|cc} A & B_1 & B_2\\ \hline C_1 & D_{11} & D_{12}\\ C_2 & D_{21} & D_{22}\end{array}\right] \tag{8}$$

Frequency Shaping by Modal Weighting Coefficient

This study proposes the simple method for frequency shaping in which modal control is realized by multiplying the modal weighting coefficient of each mode. In this method, the controlled variable of Eq. (4) is described using the following weighted modal matrix Φ_w instead of the modal matrix Φ of Eq. (2):

$$\Phi_w = [w_1\phi_1, w_2\phi_2, \ldots, w_g\phi_g] \tag{9}$$

Using this Φ_w, the controlled variable z_s can be obtained as

$$\begin{aligned} z_s &= z_s(\Phi_w)\\ &= C_{1s}(\Phi_w)q_s + D_{11s}w + D_{12s}u \end{aligned} \tag{10}$$

The modal control system is easily designed only if the modal weighting coefficients are given, and this method can reduce the order of the controller. A relatively large value must be given as the weighting coefficient of the natural mode that it is intended to suppress. From the described procedure, it is clear that this approach does not extend the order of the controller, so this modal control can be performed with a controller of small order.

Theoretical Background of Integrated Optimum Design

The H^∞ control problem in the integrated optimum design is defined. This study considers two kinds of frequency shaping methods. One is a method based on the typical frequency weighting functions, and the other is the method using the modal weighting coefficients proposed in this paper. In case of the frequency weighting functions, the H^∞ control problem can be described as

$$\left\| \begin{matrix} \gamma W_1 T_{z'w}\\ W_2 T_{uw}\end{matrix} \right\|_\infty < 1 \tag{11}$$

where $T_{z'w}$ is the transfer function matrix, between the disturbance w and the controlled response z' and T_{uw} is one between w and the control inputs u. W_1 and W_2 are the frequency weighting functions with respect to the controlled response and the control input, respectively.

In the case of the modal weighting coefficient method, the H^∞ control problem becomes

$$\left\| \begin{matrix} \gamma T_{z'_x w}\\ W_2 T_{uw}\end{matrix} \right\|_\infty < 1 \tag{12}$$

where $T_{z'_x w}$ is the transfer function matrix between the disturbance w and the weighted response z'_x obtained by Eq. (10). In the preceding H^∞ control problems, γ in Eqs. (11) and (12) should be maximized to realize the desired frequency response shaping. In this study, the

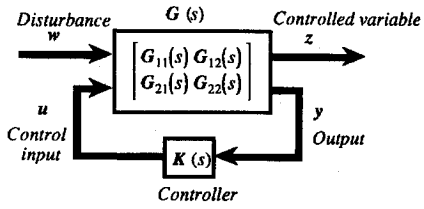

Fig. 1 Block diagram of H^∞ control system.

optimum solution to maximize γ is determined by the complex method and the GA approach.

H^∞ Control Theory

H^∞ control theory[12,13] is presented simply here to describe the integrated optimization problem. An H^∞ control system is shown in Fig. 1. The standard H^∞ control problem is concerned with constructing a dynamic feedback, internally stabilizing controller $\boldsymbol{u} = K(s)\boldsymbol{y}$ to minimize the H^∞ norm of the transfer function from $\boldsymbol{w}$ to $\boldsymbol{z}$:

$$\|T_{zw}\|_\infty < \gamma \tag{13}$$

Usually, γ is initially given and minimized by the γ-iteration process.

The H^∞ controller is designed by the two-Riccati equation formulas in this study.[12,13] The simple case in which the following equations are satisfied is taken here without loss of generality:

$$D_{11} = 0, \qquad D_{22} = 0, \qquad D_{12} = \begin{bmatrix} 0 \\ I \end{bmatrix}$$
$$D_{21} = [0 \quad I], \qquad D_{12}^T C_1 = 0, \qquad B_1 D_{12}^T = 0 \tag{14}$$

In this case, the two-Riccati H^∞ theory is applied and the solutions of two-Riccati equations are described as follows:

$$X = \mathrm{Ric}\{H_X\}, \qquad Y = \mathrm{Ric}\{H_Y\} \tag{15}$$

where H_X and H_Y are the following Hamiltonian matrices:

$$H_X = \begin{bmatrix} A & \frac{1}{\gamma^2} B_1 B_1^T - B_2 B_2^T \\ -C_1^T C_1 & -A^T \end{bmatrix} \tag{16}$$

$$H_Y = \begin{bmatrix} A^T & \frac{1}{\gamma^2} C_1^T C_1 - C_2^T C_2 \\ -B_1 B_1^T & -A \end{bmatrix} \tag{17}$$

The set of H^∞ controllers is nonempty if and only if the Riccati solutions X and Y exist and satisfy the following three conditions:

$$X \geq 0, \qquad Y \geq 0, \qquad \lambda_{\max}(XY) \leq \gamma^2 \tag{18}$$

where $\lambda_{\max}(XY)$ denotes the maximum eigenvalue of the matrix XY. If Eq. (18) is satisfied, the central solution $K(s)$ in the set of the H^∞ controller can be obtained as the following state equation:

$$\dot{\boldsymbol{x}}_k = A_k \boldsymbol{x}_k + B_k \boldsymbol{y} \tag{19}$$

$$\boldsymbol{u} = C_k \boldsymbol{x}_k \tag{20}$$

where

$$A_k = A + (1/\gamma^2) B_1 B_1^T X - B_k C_2 + B_2 C_k \tag{21}$$

$$B_k = [Y^{-1} - (1/\gamma^2) X]^{-1} C_2^T \tag{22}$$

$$C_k = -B_2^T X \tag{23}$$

The given formulation is constrained by Eq. (14), but it is clear that Eq. (14) is not always satisfied in all cases. In the case that Eq. (14) is not satisfied, the H^∞ controller can be obtained by the loop shifting method formulated by Safonov and Limebeer.[13]

Integrated Design by Complex Method

The optimization problem is defined with the following condition that the objective function becomes equal to γ in Eq. (11) or (12) under the constraint of the structural mass:

$$\begin{aligned} &\max J = \gamma \\ &\text{subj } M_{\min} \leq M \leq M_{\max} \end{aligned} \tag{24}$$

where $M_{\min}$ and $M_{\max}$ are the lower and the upper bounds of the structural mass, respectively. The thickness of the FEM element is adopted as the design variable $\tau \in \boldsymbol{R}^l$ of the structure. On the other hand, γ in Eq. (11) or (12) is adopted as the design variable with respect to the control system, as well as the objective function. The optimization is done by maximizing the γ in Eq. (24).

The existence of the H^∞ controller described in Eq. (18) must be considered in the optimization problem. The necessary and the sufficient condition for existence of the Riccati solutions X and Y is that H_X and H_Y should have no pole on the complex axis of s plane. This condition can be written using the poles s_{Xi} and s_{Yi} of the matrices H_X and H_Y as the following equations:

$$|\mathrm{Re}\{s_{Xi}\}| > 0 \qquad (\forall i) \tag{25}$$

$$|\mathrm{Re}\{s_{Yi}\}| > 0 \qquad (\forall i) \tag{26}$$

where $\mathrm{Re}\{s_{Xi}\}$ denotes the real part of the complex eigenvalue s_{Xi}. In Eq. (18), $X \geq 0$ and $Y \geq 0$ are satisfied if the eigenvalues λ_{Xi} and λ_{Yi} of the matrices X and Y satisfy the following equations:

$$\lambda_{Xi} \geq 0 \qquad (\forall i) \tag{27}$$

$$\lambda_{Yi} \geq 0 \qquad (\forall i) \tag{28}$$

In addition, $\lambda_{\max}(XY) < \gamma^2$ should be satisfied, and the design variables of both structure and control system are constrained by the upper and the lower bounds,

$$\tau^{\min} \leq \tau \leq \tau^{\max} \tag{29}$$

$$\gamma^{\min} \leq \gamma \leq \gamma^{\max} \tag{30}$$

Under these constraints, the optimum solution of the design variables to maximize the objective function of Eq. (24) is determined. Typical nonlinear optimization methods using the derivatives of the objective function can not be applied in this case because the constraints of Eq. (18) cannot be formulated as the continuous function with respect to the design variables. Therefore, the optimum solution of the design variables is searched by the complex method,[14] which is one of the random search methods, without using the derivatives of the objective function.

Integrated Design by Genetic Algorithm

The structural thickness and the locations of both sensors and actuators are adopted as the design variables. The locations of the sensors and the actuators take discrete values, because they can only be at the nodal points of the finite element model. GA is available to search for the optimum solution of the design variables in such a discrete optimization problem as this. GA consists of three basic operations, namely, selection, crossover, and mutation. In this study, the design variables are described by binary codes, and these are searched by GA for their optimum values. The structure and the control system are simultaneously optimized by this approach.

The γ in Eq. (11) or (12) is adopted as the objective function. The objective function is maximized under the constraint of the constant structural mass. The γ is also adopted as the fitness function in GA. In this approach, the fitness function f is defined as the following equation:

$$f = \begin{cases} \gamma - \gamma_0 & (\text{solvable with } \gamma \geq \gamma_g) \\ 0 & (\text{unsolvable with } \gamma = \gamma_g) \end{cases} \tag{31}$$

where γ_g is the initial value of γ, and γ_0 is introduced to leave the structural design variable that has good characteristics, when the H^∞ control problem cannot be solved.

The genetic operation in this approach is based on simple GA, and the appropriate condition of GA operation is set: namely, 1) the selection is based on the roulette selection strategy, 2) one-point crossover is adopted as the crossover strategy, in which the crossover probabilities with respect to the locations of the sensors and the actuators and with respect to the structural shape are independently defined, 3) the mutation strategy is performed by inversion of a gene that is stochastically selected, and 4) the elitist preserving strategy is adopted to leave the large fitness individuals to the next generation.

Simulation and Experiment

Approach by Complex Method

Figure 2 shows a steel plate panel structure with one fixed end whose vibration control system is designed by the proposed approach based on the complex method. The initial thickness of this plate is 3 mm and the initial mass of the structure is 2.179 kg. The striped region in Fig. 2 shows the fixed end of the plate. This plate is divided into 108 nodal points and 88 elements to make the FEM model. The displacement and the velocity in the direction normal to the surface are measured at two points (61 and 93), and the detected outputs include the sensor noises as disturbances. The detected signals are fed into the digital signal processor (DSP32C from AT&T) after A/D transformation, and necessary computation for H^∞ control is performed with the sampling frequency of 5 kHz. After D/A transformation, the output signals are fed to the two voice coil actuators attached at points 52 and 74. The disturbance forces are also applied at points 52 and 74. Thus, the disturbance vector $\boldsymbol{w}$, the output vector $\boldsymbol{y}$, and the control input vector $\boldsymbol{u}$ become

$$\boldsymbol{w} = \{w_{52}, w_{74}, w_{x61}, w_{x93}, w_{\dot{x}61}, w_{\dot{x}93}\}^T \tag{32}$$

$$\boldsymbol{y} = \{x_{61}, x_{93}, \dot{x}_{61}, \dot{x}_{93}\}^T + [\boldsymbol{0} \quad \boldsymbol{I}_4]\boldsymbol{w} \tag{33}$$

$$\boldsymbol{u} = \{u_{52}, u_{74}\}^T \tag{34}$$

The controlled variables are the displacements at the points 61, 93, and 97, and the control inputs at the points 52 and 74,

$$z_s = \{x_{61}, x_{93}, x_{97}, u_{52}, u_{74}\}^T \tag{35}$$

The frequency response function (FRF) of the initial structure between the disturbance w_{52} and the displacement x_{61} without control is shown in Fig. 3. In Fig. 3, it is observed that the calculated result agrees well with the experimental result. The five resonance peaks in the frequency range lower than 300 Hz are considered in the optimum design of the structure and the H^∞ controller. Thus, the number of the adopted modes of the structure is 5 and the order of the state equation becomes 10.

Here, the integrated design is performed by the complex method using the modal weighting coefficient to realize the modal vibration control system. The objective of the integrated design is the vibration

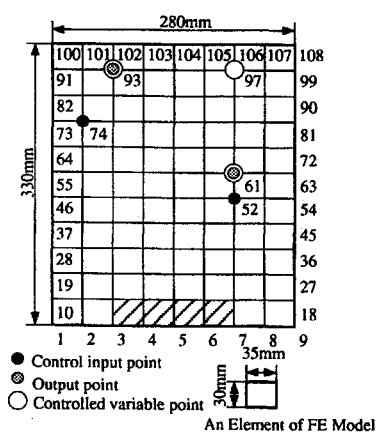

Fig. 2 Panel structure as controlled object.

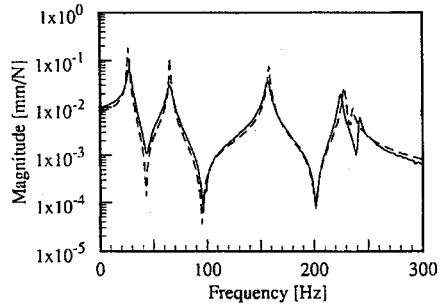

Fig. 3 FRF between w_{52} and x_{61} without control: ——, measured FRF without control; and - - -, calculated FRF without control.

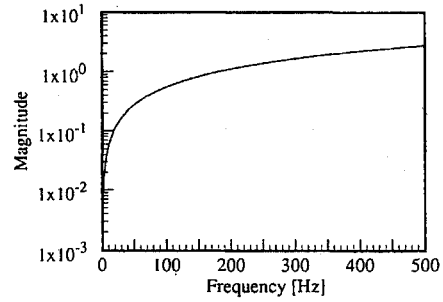

Fig. 4 FRF of the frequency weighting function $W_{e2}(s)$.

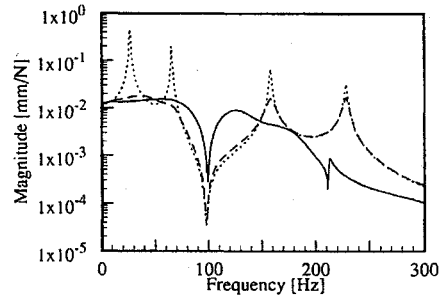

Fig. 5 FRF between w_{52} and x_{93} after optimum design by complex method: ....., calculated FRF without control; - - -, calculated FRF after controller optimization; and ——, calculated FRF after integrated optimization.

suppression of the five natural modes, especially fourth and fifth modes. The weighting coefficients are defined as

$$w_1 = 1.0, \qquad w_2 = 1.0, \qquad w_3 = 2.0$$
$$w_4 = 3.0, \qquad w_5 = 3.0 \tag{36}$$

The frequency weighting function W_2 with respect to the control input is introduced as the following equation to maintain stability robustness in the presence of the structural uncertainty:

$$W_2 = \mathrm{diag}[w_{e2}(s), w_{e2}(s)]$$
$$w_{e2}(s) = 20s/(s + 2.262 \times 10^4) \tag{37}$$

The FRF of Eq. (37) is shown in Fig. 4. In this case, γ in Eq. (12) is adopted as the objective function and is maximized by the presented approach based on the complex method.

First, the design of only the control system without the structural optimization is performed by γ-iteration procedure. As the result, the maximum value of γ becomes 2.4827 and the controlled FRF between w_{52} and x_{93} is shown in Fig. 5 by the broken line. It is observed in Fig. 5 that the vibration of the low-order modes is largely suppressed but the high-order resonance peaks cannot be suppressed sufficiently.

Next, the integrated design of the structure and the control system presented in this study is performed. The structural design variables are the thicknesses of the five regions, as shown in Fig. 6, all of which are bounded to take the values between 1.5 and 4.5 mm. The objective function is $J = \gamma$ and the mass M of the structure is

Table 1 Optimum values of structural thickness obtained by complex method

Region no.	1	2	3	4	5
Thickness, mm	1.83	1.66	4.38	4.11	2.92

Total mass of the structure = 2.167 [kg]

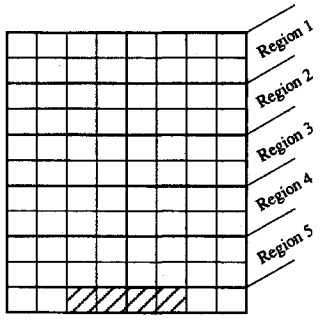

Fig. 6 Regions of structural design variable.

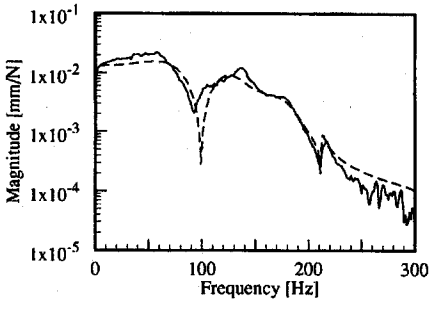

Fig. 7 Experimental result of FRF between w_{52} and x_{93}: - - - -, calculated FRF after integrated optimization; and ——, measured FRF after integrated optimization.

constrained as 2.0 kg $\leq M \leq$ 2.2 kg to prevent a large change of the mass from the initial structure. The modal weighting coefficient and the frequency weighting function of the control input are the same as Eqs. (36) and (37). As the result of the integrated design, the maximum γ becomes 4.9295 and the structural mass M is changed to 2.167 kg. The optimum solution of the thickness is shown in Table 1. The value of the maximum γ in the integrated design becomes larger than that in the control system only design. The FRF calculation result between w_{52} and x_{93} is shown in Fig. 5 by the solid line. It is clear from this figure that the higher mode vibration for the integrated design is suppressed more than for the control-only design . The experimental result of FRF for the integrated design is shown in Fig. 7 by the solid line. In Fig. 7, the broken line is the calculated result that agrees well with the experimental one.

Approach by Genetic Algorithm

In this approach based on GA, the thickness of the FEM model and the locations of where the sensors and the actuators are attached are taken as the design variables. The controlled object is the panel structure, which is the same one as shown in Fig. 2. In this case, the disturbances act at points 53 and 74, and the displacements at points 60, 92, and 98 are evaluated as the controlled variables, as shown in Fig. 8. The design variables are the thicknesses of five regions in Fig. 6, all of which are bounded to take the values between 1.5 and 4.5 mm, and the locations of where the 2 sensors and the 2 actuators are attached.

The control input vector $\boldsymbol{u}$, the disturbance vector $\boldsymbol{w}$, the output vector $\boldsymbol{y}$ and the controlled variable vector $\boldsymbol{z}$ are defined by the following equations:

$$\boldsymbol{u} = \{u_1, u_2\}_s^T \tag{38}$$

$$\boldsymbol{w} = \{w_{53}, w_{74}, w_{nd1}, w_{nd2}, w_{nv1}, w_{nv2}\}^T \tag{39}$$

$$\boldsymbol{y} = \{y_1, y_2, \dot{y}_1, \dot{y}_2\}^T + 10.0 \times [0 \quad \boldsymbol{I}_4]\boldsymbol{w} \tag{40}$$

$$\boldsymbol{z}_s = \{x_{60}, x_{92}, x_{98}, u_1, u_2\}^T \tag{41}$$

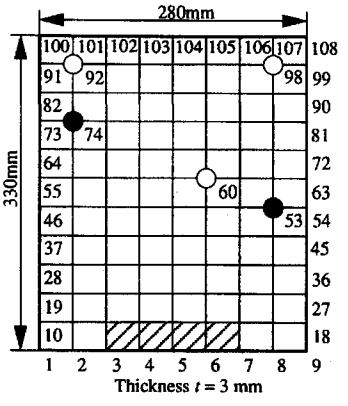

Fig. 8 Disturbance input and controlled variable points: •, disturbance input points; and ○, controlled variable points.

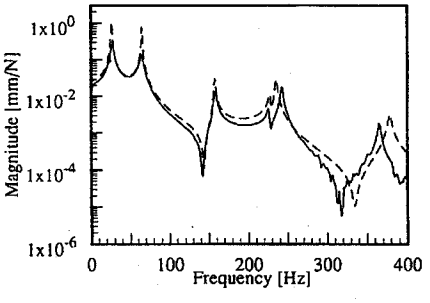

Fig. 9 FRF between w_{53} and x_{92} without control: - - - -, calculated FRF without control; and ——, measured FRF without control.

where w_{ndi} and w_{nvi} are the output noises with the displacement and the velocity sensors, respectively, whose attachment locations are optimized in this approach.

FRF between w_{53} and x_{92} without control is shown in Fig. 9 in which the broken line is the calculation result and the solid line is the experimental result, respectively. The number of the adopted modes is five here, as well as the preceding case.

The design variables should be coded to search the optimum solution by GA. In this approach, the design variables are described by binary code with 39 bits:

$$\underbrace{t_1 t_2 \ldots t_6}_{\text{actuator 1}} \quad \underbrace{t_7 \ldots t_{12}}_{\text{actuator 2}} \quad \underbrace{t_{13} \ldots t_{18}}_{\text{sensor 1}} \quad \underbrace{t_{19} \ldots t_{24}}_{\text{sensor 2}} \quad \underbrace{t_{25} \ldots t_{39}}_{\text{structure}} \tag{42}$$

where t_i shows the genes, all of which can take the values of 0 or 1. The symbols t_1–t_6 indicate the nodal point number with the binary code for the location where one of the actuators should be attached, and that nodal point number m becomes

$$m = \begin{cases} \left(2^2 \times t_1 + 2^1 \times t_2 + 2^0 \times t_3\right) \times 9 \\ \quad + \left(2^1 \times t_5 + 2^0 \times t_6\right) + 37 & (t_4 = 0) \\ \left(2^2 \times t_1 + 2^1 \times t_2 + 2^0 \times t_3\right) \times 9 \\ \quad - \left(2^1 \times t_5 + 2^0 \times t_6\right) + 37 & (t_4 = 1) \end{cases} \tag{43}$$

The location of the other actuator and the two sensors are also defined in the same way as Eq. (43).

The t_i from t_{25}–t_{39} show the structural thicknesses of the five regions with the binary code. Each thickness is described by each binary code with 3 bits,

$$\underbrace{t_{25} t_{26} t_{27}}_{\text{region 1}} \quad \underbrace{t_{28} t_{29} t_{30}}_{\text{region 2}} \quad \underbrace{t_{31} t_{32} t_{33}}_{\text{region 3}} \quad \underbrace{t_{34} t_{35} t_{36}}_{\text{region 4}} \quad \underbrace{t_{37} t_{38} t_{39}}_{\text{region 5}} \tag{44}$$

Thus, each thickness τ_i can take one of the following discrete values (in millimeters):

$$\tau_i = 1.5, 2.0, 2.5, 3.0, 3.5, 4.0, 4.5 \tag{45}$$

For example, one thickness τ_1 of the region 1 is given as the following equation:

$$\tau_1 = 0.5 \times \left(2^0 \times t_{25} + 2^1 \times t_{26} + 2^2 \times t_{27}\right) + 1.5 \tag{46}$$

Table 2 Parameters in integrated design by GA

	Actuator	Sensor	Structure
Population size	60	60	60
Chromosome length	12	12	15
Selection probability, %	80	80.0	80
Crossover probability, %	60.0	60.0	60.0
Mutation probability, %	1.0	1.0	1.0

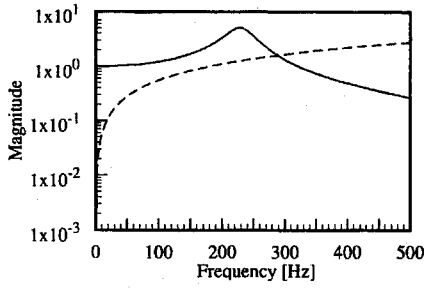

Fig. 10 FRFs of frequency weighting functions: ——, W_{e1}; and - - - -, W_{e2}.

The thicknesses from region 2 to region 5 are found in the same way as Eq. (46). However, no chromosome takes the thickness $\tau_i = 5$ mm in this optimization algorithm.

Here, the integrated design based on the frequency weighting functions is performed to realize the desired frequency shaping. The following frequency weighting functions are defined:

$$z = W(s)z_s \tag{47}$$

$$W(s) = \mathrm{diag}(W_{e1} \cdot \gamma,\ W_{e1} \cdot \gamma,\ W_{e1} \cdot \gamma,\ W_{e2},\ W_{e2}) \tag{48}$$

$$W_{e1}(s) = \frac{2.088 \times 10^6}{s^2 + 289.0s + 2.088 \times 10^6} \tag{49}$$

$$W_{e2}(s) = \frac{20.00s}{s + 2.262 \times 10^4} \tag{50}$$

$$W_1(s) = \mathrm{diag}(W_{e1},\ W_{e1},\ W_{e1}) \tag{51}$$

$$W_2 = (W_{e2},\ W_{e2}) \tag{52}$$

FRFs of these frequency weighting functions are shown in Fig. 10, in which the solid line is the weighting function with respect to the vibration response and the broken line is that with respect to the control input. The objectives of the integrated optimum design are vibration reduction near 230 Hz close to the fourth and fifth resonance peaks of the original structure, and the achievement of stability against the ignored higher modes. The order of the H^∞ controller becomes 18, which is larger than the preceding case using the modal weighting coefficients. In this case, γ in Eq. (11) is adopted as the fitness function and is maximized by the presented approach by GA.

In the integrated design by GA, γ_0 and γ_g in Eq. (31) are defined as

$$\gamma_0 = 0.125, \qquad \gamma_g = 0.125 \tag{53}$$

The mass of the structure is constrained to be $M = 2.179$ kg, which is the initial mass of the structure. The parameters in the integrated design by GA are shown in Table 2. The integrated optimum design is done using the four kinds of random numbers, and the result of the optimum fitnesses obtained by the presented approach is shown in Table 3. Each design variable of the result 1 in Table 3 is shown in Table 4. FRFs between w_{53} and x_{98}, and between w_{74} and x_{98} calculated by the result 1 are shown in Figs. 11 and 12, respectively. In Figs. 11 and 12, the dotted lines are FRF without control, the broken lines are the results after the optimization of only the locations of the sensor and the actuator, and the solid lines are FRF after the integrated optimum design. It is observed from Figs. 11 and 12 that the vibration response near 230 Hz is strongly suppressed in the integrated optimum design.

It is easily understood that the modal vibration control and the reduction of the controller using the modal weighting coefficients

Table 3 Result of optimum fitness obtained by integrated design

	Optimum fitness		Average fitness	
	1st generation	50th generation	1st generation	50th generation
Result 1	3.344	7.234	0.955	5.704
Result 2	3.148	6.641	0.972	4.502
Result 3	4.000	6.914	0.941	4.905
Result 4	4.063	6.188	1.003	4.520

Table 4 Result of each design variable by result 1 in Table 3

	Node no. of actuator		Node no. of sensor		
Fitness	101	98	103	91	
	Region 1	Region 2	Region 3	Region 4	Region 5
7.234	4.0 mm	3.5 mm	4.0 mm	1.5 mm	2.0 mm

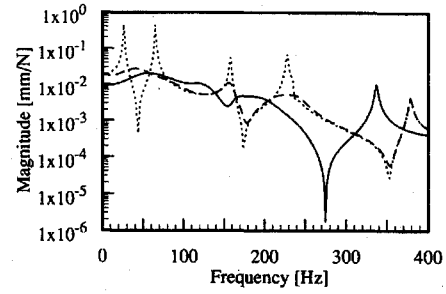

Fig. 11 FRF between w_{53} and x_{98} after optimum design by GA: ....., calculated FRF without control; - - - -, calculated FRF after sensor and actuator placement optimization; and ——, calculated FRF after integrated optimization.

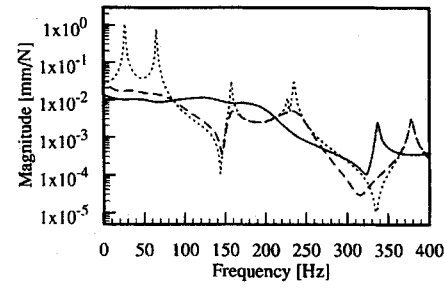

Fig. 12 FRF between w_{74} and x_{98} after optimum design by GA: ....., calculated FRF without control; - - - -, calculated FRF after sensor and actuator placement optimization; and ——, calculated FRF after integrated optimization.

can be realized with the GA approach, as well as with the complex method. The results obtained in the described applications indicate that high-performance frequency response shaping can be realized by the proposed integrated optimum design of the structure and the H^∞ control system.

Conclusions

1) Approaches to the problem of an integrated optimum design of a structure and an H^∞ control system based on complex method and GA are proposed to realize high-performance frequency response shaping.

2) An excellent improvement of the frequency response shaping under the constraint of the structural mass can be realized by the approaches to integrated optimum design proposed in this paper.

3) The optimum design with the discontinuous constrained functions with respect to H^∞ controller existence is achieved by the

complex method, and the structural shape and the H^∞ control system, including the locations of both sensors and actuators, can be simultaneously optimized by the GA approach.

4) The frequency response shaping method using the modal weighting coefficient is available to control each mode and prevents an increase of the order of the controller.

5) Validity and usefulness of the proposed approaches are verified by both simulation and experiment.

References

[1]Salama, M., Garba, J., and Demsetz, L., "Simultaneous Optimization of Controlled Structures," *Computational Mechanics*, Vol. 3, No. 4, 1988, pp. 275–282.

[2]Milman, M., Salama, M., Scheid, R. E., Bruno, R., and Gibson, J. S., "Combined Control-Structural Optimization," *Computational Mechanics*, Vol. 8, No. 1, 1991, pp. 1–18.

[3]Khot, N. S., and Venkayya, V. B., "Optimal Structural Modifications to Enhance the Active Vibration Control of Flexible Structures," *AIAA Journal*, Vol. 24, No. 8, 1986, pp. 1368–1374.

[4]Venkayya, V. B., Tischler, V. A., and Khot, N. S., "Dynamics and Control of Space Structures," *Engineering Optimization*, Vol. 11, Nos. 3, 4, 1987, pp. 251–264.

[5]Miller, D. F., Venkayya, V. B., and Tischler, V. A., "Integration of Structures and Controls. Some Computational Issues," *Proceedings of the 24th IEEE Conference on Decision and Control* (Fort Lauderdale, FL), Vol. 24, No. 2, Inst. of Electrical and Electronics Engineers, 1985, pp. 924–931.

[6]Junkins, J. L., and Rew, D. W., "A Simultaneous Structure/Controller Design Iteration Method," *IEEE Proceedings of the American Control Conference*, Vol. 3, American Automatic Control Council, Boston, MA, 1985, pp. 1642–1647.

[7]Bodden, D. S., and Junkins, J. L., "Eigenvalue Optimization Algorithms for Structure/Controller Design Iterations," *Journal of Guidance, Control, and Dynamics*, Vol. 8, No. 6, 1985, pp. 697–706.

[8]Haftka, R. T., Martinovic, Z. N., Hallauer, W. L., Jr., and Schamel, G., "An Analytical and Experimental Study of a Control System's Sensitivity to Structural Modifications," *AIAA Journal*, Vol. 25, No. 2, 1987, pp. 310–315.

[9]Onoda, J., and Haftka, R. T., "An Approach to Structure/Control Simultaneous Optimization for Large Flexible Spacecraft," *AIAA Journal*, Vol. 25, No. 8, 1987, pp. 1133–1138.

[10]Kajiwara, I., Tsujioka, K., and Nagamatsu, A., "Approach for Simultaneous Optimization of a Structure and Control System," *AIAA Journal*, Vol. 32, No. 4, 1994, pp. 866–873.

[11]Khot, N. S., and Öz, H., "Structural-Control Optimization with H_2 and H_∞ Constraints," *Proceedings of the 34th Structural Dynamics and Materials Conference*, AIAA, Washington, DC, 1993, pp. 1429–1437 (AIAA Paper 93-1470).

[12]Doyle, J. C., Glover, K., Khargonekar, P. P., and Francis, B. A., "State-Space Solutions to Standard H_2 and H_∞ Control Problems," *IEEE Transactions on Automatic Control*, Vol. 34, No. 8, 1989, pp. 831–847.

[13]Safonov, M. G., and Limebeer, D. J. N., "Simplifying the H^∞ Theory via Loop Shifting," *Proceedings of the 27th Conference on Decision and Control* (Austin, TX), Inst. of Electrical and Electronics Engineers, 1988, pp. 1399–1404.

[14]Rao, S. S., *Optimization Theory and Applications*, Wiley Eastern, New Delhi, India, 1984, pp. 345–348.